ORNL/TM-6360

Performance of a Modified DuoPIGatron Ion Source for PLT Neutral Beam Injectors

C. C. Tsai
W. L. Stirling
H. H. Haselton
D. E. Schechter
G. C. Barber
W. K. Dagenhart
R. C. Davis
W. L. Gardner
M. M. Menon
N. S. Ponte
P. M. Ryan
J. H. Whealton
R. E. Wright

OAK RIDGE NATIONAL LABORATORY
OPERATED BY UNION CARBIDE CORPORATION · FOR THE DEPARTMENT OF ENERGY

ORNL/TM-6360
Dist. Category UC-20 a

Contract No. W-7405-eng-26

FUSION ENERGY DIVISION

Performance of a Modified DuoPIGatron Ion Source for PLT Neutral Beam Injectors

C. C. Tsai, W. L. Stirling, H. H. Haselton, D. E. Schechter,
G. C. Barber, W. K. Dagenhart, R. C. Davis, W. L. Gardner,
M. M. Menon, N. S. Ponte, P. M. Ryan, J. H. Whealton,
and R. E. Wright

Date Published - September 1978

NOTICE This document contains information of a preliminary nature. It is subject to revision or correction and therefore does not represent a final report.

Prepared by the
OAK RIDGE NATIONAL LABORATORY
Oak Ridge, Tennessee 37830
operated by
UNION CARBIDE CORPORATION
for the
DEPARTMENT OF ENERGY

CONTENTS

ABSTRACT

The performance of a modified duoPIGatron ion source for PLT neutral beam injectors is described. The 22-cm source has been operated to deliver beams of 70 A, up to 45 keV, and 0.5 sec. Following a brief review of source operation, the dominant reactions leading to an enhanced atomic ion fraction in the source plasma are emphasized. In addition to the high atomic ion species yield (about 85%), other important characteristics of the source such as high arc efficiency (about 1.1 A ion beam current per kW of arc power), long filament lifetime, high reliability, and scalability are also described.

1. INTRODUCTION

Recent experimental results involving neutral beam injection heating of tokamak plasmas[1-4] have demonstrated the efficiency and scalability of this heating technique. Typical ion temperatures of 0.5-1.0 keV are achieved by applying only ohmic heating. For example, the injection of ∿1 MW of neutral power into PLT raised the ion temperature from ∿1 keV to ∿2.3 keV.[4] This encourages the use of multimegawatt neutral beams for the present and next generation fusion devices,[5-7] such as Princeton Large Torus (PLT), Poloidal Divertor Experiment (PDX), and Tokamak Fusion Test Reactor (TFTR) at Princeton Plasma Physics Laboratory (PPPL), Doublet III at General Atomic (GA), and Impurity Study Experiment (ISX) at Oak Ridge National Laboratory (ORNL).

Usually an ion source with hydrogen or its isotopes as a working gas creates a plasma that consists of atomic and molecular positive ions. Resulting neutral beams have three major energy components: E, E/2, and E/3. Such a neutral beam with multienergy components tends to heat the outer edge of tokamak plasma causing sputtering impurities from the wall and impairing the effect of plasma heating. By eliminating all but one energy species, the particles of the neutral beam can effectively penetrate the plasma center, thereby heating the plasma with high efficiency and avoiding deleterious impurities.[8] An ion source such as the modified duoPIGatron, with the capability to enhance one of the three hydrogen ion species (presently the atomic species), is suitable for use in efficient high power neutral injection systems.

The plasma heating experiments on PLT at PPPL require a 1-MJ neutral beam of energetic hydrogen particles.[9] To fulfill this challenging goal, four neutral beam lines designed with the capability of producing ion beams of 60-A current, 40-keV ion energy, and 300-ms pulse length have been successfully developed at ORNL. The use of these beam lines demonstrates the compatibility of the modified duoPIGatron ion source and the other parallel systems such as electronics associated with arc and high voltage power supplies, gas feed system, cryopumping system, and transport systems.

BLANK PAGE

For the PLT neutral injector design, the duoPIGatron (31-cm anode 2 chamber diameter and 22-cm grid diameter) is modified with an arrangement of permanent magnets forming a multipole line cusp magnetic field. The cusp field improves confinement of both ionizing electrons and plasma created in the anode region. Consequently, the source efficiently creates a more uniform, dense plasma over the entire grid area.[10] It has been operated reliably to deliver hydrogen ion beams with currents up to 70 A, ion energies up to 45 keV, and pulse lengths up to 500 ms. As indicated in Table 1, the source is also characterized with high arc efficiency (∿1.1 A ion beam current per kW of arc power), high proton yield (∿85%), long filament lifetime (over 50,000 pulses without deterioration), high reliability, and scalability. In the following sections, the source operation is briefly reviewed and the dominant reactions for the high proton yield are then emphasized.

2. SOURCE OPERATION

Figure 1 shows a sketch of a modified duoPIGatron ion source. As in a conventional duoPIGatron,[11] it consists of filaments, intermediate electrodes, anodes, and the extraction electrodes. In addition, on the outside walls of the anode 2 chamber, there are 20 permanent magnet columns about 17.5 cm long. With an alternating polarity in the azimuthal direction of the adjacent columns, a multipole magnetic line cusp field is established in the anode 2 region with a peak value of ∿2000 G at the anode 2 surface.

During normal operation (see Table 2), the source plasma is composed of a cathode plasma in the intermediate electrode chamber and an anode (or PIG) plasma in the anode 2 chamber. The assembly of oxide filaments, intermediate electrode, and the cathode plasma work as a hollow cathode to supply prime ionizing electrons to the anode region. These electrons follow the inhomogeneous magnetic field lines which originate at the intermediate electrode and spread out in the anode region. The anode region extends from the intermediate electrode to the target cathode. On their way from the intermediate electrode to the target cathode, the fast electrons (∿100 eV) create an anode plasma. With the improved confinement for charged particles due to the line cusp magnetic field, they efficiently create a dense, uniform plasma at the target cathode grid (±5% current density variations over the whole grid). An ion beam is then extracted from this high quality plasma and accelerated. Passing through the hydrogen gas neutralization cell, a portion of the ion beam is converted into a neutral beam.

3. ION SPECIES

In a hydrogen plasma, there are atomic ions (H_1^+) and molecular ions (H_2^+ and H_3^+). Considering penetration of a neutral beam into the tokamak plasma, it is preferable to enhance a single ion fraction in the source. The atomic ion fraction is the easiest to maximize. In addition to the thermal predissociation of hydrogen gas,[12] electron dissociation in the discharge is an effective way to enhance proton yield in an ion source. This latter process, as elaborated below, supports the measured high value of proton yield (∿85%) in the PLT-type source.

The ion species ratio in the PLT-type source was measured as follows. In the neutral beam line, a deflection magnet is installed downstream at the end of the gas cell for deflecting the unneutralized ions to the corresponding ion dumps. The power measured on the ion dumps is used for determination of the ion species fractions in the source. To adjust the correct magnetic field strength for a given ion energy, we have installed Langmuir probes in various ion dumps. Moreover, to improve the accuracy of the measurement, single-swirl-tube calorimeter probes (one for each ion dump) are also employed.

Data are acquired by using one of two methods: (1) using one probe for each species at an appropriate bending magnetic field strength, or (2) using one probe for three species at different strengths of bending field. The experimental results obtained from method 2 and shown in Fig. 2, reveal the high value of proton yield in the source. For example, the beam fraction ratio at the ion source for various ion species is $J_1:J_2:J_3 = 85:12:3$; J_1 is for H_1^+, J_2 is for H_2^+, and J_3 is for H_3^+.

Based on electron dissociation, Bromberg[13] predicts a proton yield of 75% in a modified duoPIGatron. In fact, we have measured proton yields as high as 85%. To find the governing factors for this high proton yield, we have conducted a theoretical study. A species model has been developed which is based on the discharge mechanism and prime reactions relevant to the production and loss of hydrogen ions in the modified duoPIGatron as described below.

In a modified duoPIGatron ion source,[11] ions extracted are supplied from the anode plasma adjacent to the extraction electrodes. The anode plasma is created essentially by the hot electrons which are accelerated into the anode region from the cathode plasma. The density of hot electrons can be determined and is briefly described below. If we assume that all the hot electrons passing through the anode 1 region spread uniformly over the surface of the target cathode for a case of 600-A arc current and 100-eV electron energy, the hot electron density is about 10^{11} cm^{-3} in the anode 1 region and about 9×10^{9} cm^{-3} in the target cathode region. In fact, the gas pressure in the anode region is $\sim$15 mTorr and the distance between the anode 1 and target cathode is as long as 25 cm. It is expected that only about 10% or less of hot electrons (without colliding with hydrogen particles) can arrive at the target cathode. Thus, the hot electron density is reduced to 10^{9} cm^{-3} or less at the extraction surface. Furthermore, the electron temperature measurement, using a Langmuir probe in the target cathode region, reveals that the energy of cold plasma electrons is $\sim$5 eV and the energy of primary electrons is well below 10 eV. These values can vary slightly for various arc conditions. It is clear that the ions in the anode plasma are produced by the hot electrons. Considering the density and energy variations of hot electrons in the anode region, we realize that the extracted ions from a modified duoPIGatron are created primarily in the volume of the anode plasma region, not at the target cathode surface. Hence, the high proton yield measured must be associated with a high production rate of protons in the volume plasma.

To determine the dominant reactions for creation and loss of various hydrogen ions in the volume of the anode plasma, we evaluate each reaction by utilizing the reaction rate per unit volume. As listed in the last column of Table 3, it is the product of each particle density (n_a, n_b), velocity (v), and cross section (σ), or $n_a n_b \langle \sigma v \rangle$. The magnitudes of these quantities in the volume near the anode 1 are estimated by using the following assumptions and typical values given in Table 2. The density of molecular hydrogen (N_2) is 6×10^{14} cm^{-3}. The density of hot electrons (n_h) is 4×10^{10} cm^{-3}. Energy of these electrons is up to 70 eV. The density of cold plasma electrons (n_c) is 9×10^{12} cm^{-3}, and the cold electron temperature is 3 eV. We assume about 0.25 eV thermal energy for protons and hydrogen atoms and 0.025 eV for molecular ions. Assuming that the H_2^+ ion density is $\sim 1.2 \times 10^{12}$ cm^{-3} and that the plasma electron density is equal to the sum of ion densities, we estimate the densities of various ions. For the cross sections σ at energy E, or $\langle \overline{\sigma v} \rangle$ in Table 3, published data[14–18] are used. In this table, H_2 is for hydrogen molecules, H_1 is for atoms, H_1^+ is for protons, H_2^+ and H_3^+ are for molecular ions, H_1^* is for excited atoms, e_h is for hot electrons, e_c is for cold plasma electrons, and e is for all electrons.

Based on the discharge conditions and dominant reactions, the anode plasma is created by the following processes. First of all, the hot electrons create H_2^+ ions at a high rate in the anode 1 region. Subsequently, most of these ions are converted via the processes of dissociative excitation, recombination, ionization, and charge exchange. The net proton generation rate in the volume excluding the charge exchange is about 80%. The rest of the protons are created by either direct ionization or excitation and ionization of hydrogen atoms. These atoms are produced essentially through two ways: (1) from cold electron dissociation of hydrogen molecules and (2) from charge exchange of molecular ions and then through electron dissociation.

By balancing the creation and loss for each species of hydrogen neutrals and ions and utilizing reaction rates per unit volume as given in Table 3, the densities of various particles in the plasma volume are calculated and given as the following:

Plasma density	$n_c \simeq 9.33 \times 10^{[illegible]}$ cm^{-3}
H_1^+ density	$n_1 \simeq 7.36 \times 10^{12}$ cm^{-3}
H_2^+ density	$n_2 \simeq 1.12 \times 10^{12}$ cm^{-3}
H_3^+ density	$n_3 \simeq 0.85 \times 10^{12}$ cm^{-3}
H_1 density	$N_1 \simeq 6.66 \times 10^{13}$ cm^{-3}

Hence, the species ratio $n_1:n_2:n_3$ = 79:12:9. The beam fraction ratio $J_1:J_2:J_3$ = 85:9.2:5.6. The excellent agreement of the calculated and measured values strongly supports the above theoretical treatment.

4. ARC EFFICIENCY

The measured arc efficiency is >1 A ion beam current per kW of arc power. This high arc efficiency is achieved by optimizing the geometrical configuration and dimensions of the electrodes, the cusp field arrangement, and source operation. In this context, anode 1 is found to be the most crucial component. It can affect both the fraction of ionizing electrons which participate in the volume processes mentioned above and the loss rate of the plasma created. Moreover, the cusp field arrangement not only enables the source to create a uniform, dense plasma but also reduces the loss rate of the prime electrons and the plasma to the surface of anode 2. Regarding the source operation, the separate gas feeds into different regions of the discharge enable the source to be operated in a high arc impedance mode. The resulting high kinetic energy of the prime ionizing electrons efficiently creates the dense anode plasma.

With both the source elements and parameters optimized, an arc efficiency of >1 A ion beam current per kW of arc power can be realized. For example, the arc power for a beam of 65 A/37 keV is about 59 kW (105 V arc voltage and 560 A arc current), i.e., 1.1 A/kW. The high efficiency is important for significant savings in the size of the arc power supply for efficient neutral beam systems.

5. FILAMENT LIFETIME

The hot cathode of this source consists of 8 filaments which are oxide coated and are arranged off axis. Each filament is capable of delivering 100 A of electron current. Hence, the arc current capability of the hot cathode exceeds the requirement of the PLT-type source. Moreover, the off-axis arrangement of the multiple filaments is designed to prolong filament lifetime by reducing bombarding damage of back-streaming energetic particles. Also, since the potential difference between the intermediate electrode and the filament is about 30 V or less, the resulting damage to the filaments due to the bombarding of ions from the cathode plasma is negligible. Consequently, the filament lifetime is very long; we have not had adequate time to determine the limit. The filament has performed without a noticeable deterioration for over 50,000 pulses. Moreover, the filament is also characterized with high ruggedness; for example, after accidents exposing them to air and water vapor during operation, the filaments still work properly.

6. RELIABILITY AND QUASI-dc OPERATION

The pulse length of a PLT-type source is designed to be 300 ms. We have run as long as 500 msec per pulse for the arc discharge. For 300 ms beam pulses with 500 kW of neutral power transmitted through a PLT beam line, about 80% of the pulses occur without interruption. With water cooling modifications to filament feedthroughs and axial button in the intermediate electrode snout, the plasma generator will have a dc capability.

7. SCALABILITY

During the last 10 years, the duoPIGatron ion source originally developed at ORNL has been successfully scaled up from 1 A to 70 A. Further scaling of the present modified duoPIGatron is relatively simple. In the last few years, the 10-cm source for the Oak Ridge Tokamak (ORMAK) neutral injectors has been scaled up to 15-cm, 20-cm, and 22-cm sources. The 15-cm injectors have been used for the

Laser Initiated Target Experiment (LITE) at United Technologies Research Center (UT) and the plasma heating experiments on ORMAK at ORNL. Several 22-cm injectors have been developed for PLT at PPPL and ISX at Oak Ridge. At the moment, we are developing 100-A (ion current) sources for ISX and PDX at PPPL. We have already operated the plasma generator (35-cm anode 2 chamber diameter), and the uniform plasma created is capable of 100 A ion beam extraction from a 26-cm diameter grid. Arc power supplies will be installed within the next year which will give us the capability of investigating sources with a beam current up to 300-A output.

8. SUMMARY

From the above text, we summarize the following significant points:

(1) The development and operation of the PLT beam lines at ORNL have demonstrated that both the ion source and other beam line subsystems form a mutually compatible working environment. Also, the ion source can be scaled up for a neutral injection system with higher power and energy.

(2) The modified duoPIGatron ion sources possess the following proven characteristics: stable and reliable operation, high proton yield, high arc efficiency, long filament lifetime, dc capability, and scalability.

(3) In addition to the high arc efficiency, the observed proton yield as high as 85% is one of the most outstanding features of the modified duoPIGatron ion sources.

(4) The species model described is valuable for the development of a hydrogen or deuterium plasma generator with a capability of species selectivity.

We conclude from our in-depth studies and long-term operation of this type ion source that it is a fully qualified candidate for future efficient high power neutral beam injectors, especially when one considers the effective penetration and deposition of beam power into tokamak plasmas.

ACKNOWLEDGMENTS

We would like to express our appreciation to S. W. Schwenterly for his assistance in upgrading the cryocondensation gas pumping system. The fruitful discussions with L. Bromberg at Massachusetts Institute of Technology, L. R. Grisham, G. Schilling, and L. D. Stewart at Princeton Plasma Physics Laboratory, and C. A. Foster, G. G. Kelley, J. Kim, S. L. Milora, and O. B. Morgan at ORNL are appreciated. Thanks are due to C. W. Blue, R. E. Potter, and D. O. Sparks for their excellent support in keeping the test facilities operational.

REFERENCES

1. O. B. Morgan et al., "The Development and Application of Neutral Injection Heating for ORMAK," invited talk given at the International School of Plasma Physics Symposium on Plasma Heating and Toroidal Devices, Varenna, Italy, September 6-17, 1976, TM 88 of the Plasma Technology Section (unpublished).

2. K. Bol et al., Phys. Rev. Lett. 32, 661 (1974).

3. TFR Group (presented by R. Dei-Cas), "Neutral Injection Heating in TFR," 3rd International Meeting on Theoretical and Experimental Aspects of Heating of Toroidal Plasmas," Grenoble, France, June 28-July 2, 1976.

4. H. P. Eubank (Princeton Plasma Physics Laboratory), 1977.

5. J. H. Willis et al., "Neutral Beam Energy and Power Requirements for the Next Generation of Tokamaks," Washington D.C. ERDA 76-77 (June 1976).

6. L. D. Stewart et al., Proc. 6th Symp. on Plasma Physics and Controlled Nuclear Fusion Research, Vol. 3, p. 293.

7. O. B. Morgan et al., "The Development of Neutral Injection Heating for Large Tokamaks and Reactors at ORNL," invited talk given at the International School of Plasma Physics Symposium on Plasma Heating and Toroidal Devices, Varenna, Italy, September 6-17, 1976, TM 89 of the Plasma Technology Section (unpublished).

8. J. A. Rome, J. D. Callen, and J. F. Clarke, Nucl. Fusion 14, 141 (1974); J. A. Rome, "Beam Penetration — Theory and Prediction," presented at the Pellet Fueling Workshop, Princeton, New Jersey, November 1-5, 1977.

9. H. H. Haselton et al., "PLT and Doublet III Neutral Beam Injection Systems," 6th Symp. on Engineering Problems of Fusion Research, San Diego, California, 1975.

10. W. L. Stirling, C. C. Tsai, and P. M. Ryan, Rev. Sci. Instrum. 48, 533 (1977); C. C. Tsai et al., Proc. 7th Symp. on Engineering Problems of Fusion Research, Vol. I, p. 533; W. K. Dagenhart et al., Proc. 7th Symp. on Engineering Problems of Fusion Research, Vol. I, p. 278.

11. C. C. Tsai, W. L. Stirling, and P. M. Ryan, Rev. Sci. Instrum. 48, 651 (1977).

12. J. Kim and R. C. Davis, Appl. Phys. Lett. 30, 130 (1977).

13. L. Bromberg, "Theory of Low Pressure Thermionic Discharges Used for Positive Ion Extraction," Ph.D. Thesis, Massachusetts Institute of Technology, May 1977.

14. C. F. Barnett et al., "Atomic Data for Controlled Fusion Research," ORNL-5206 and -5207, 1977.

15. A. R. Martin, "Reaction Cross Sections of Relevance to Hydrogen Plasma in Ion Sources," CLM-R 157, 1976.

16. A. R. Martin and T. S. Green, "Computations of Hydrogen Ion Species Produced in High Current Ion Sources," CLM-R 159, 1976.

17. D. F. Dance et al., Proc. Phys. Soc. 92, 577 (1967).

18. B. Peart and K. T. Dolder, J. Phys. B 4, 1496 (1971); J. Phys. B 5, 1554 (1972).

FIGURE CAPTIONS

Fig. 1. A sketch of 60 A duoPIGatron ion source.

Fig. 2. Calorimeter scan of the full, half, and third energy ions.

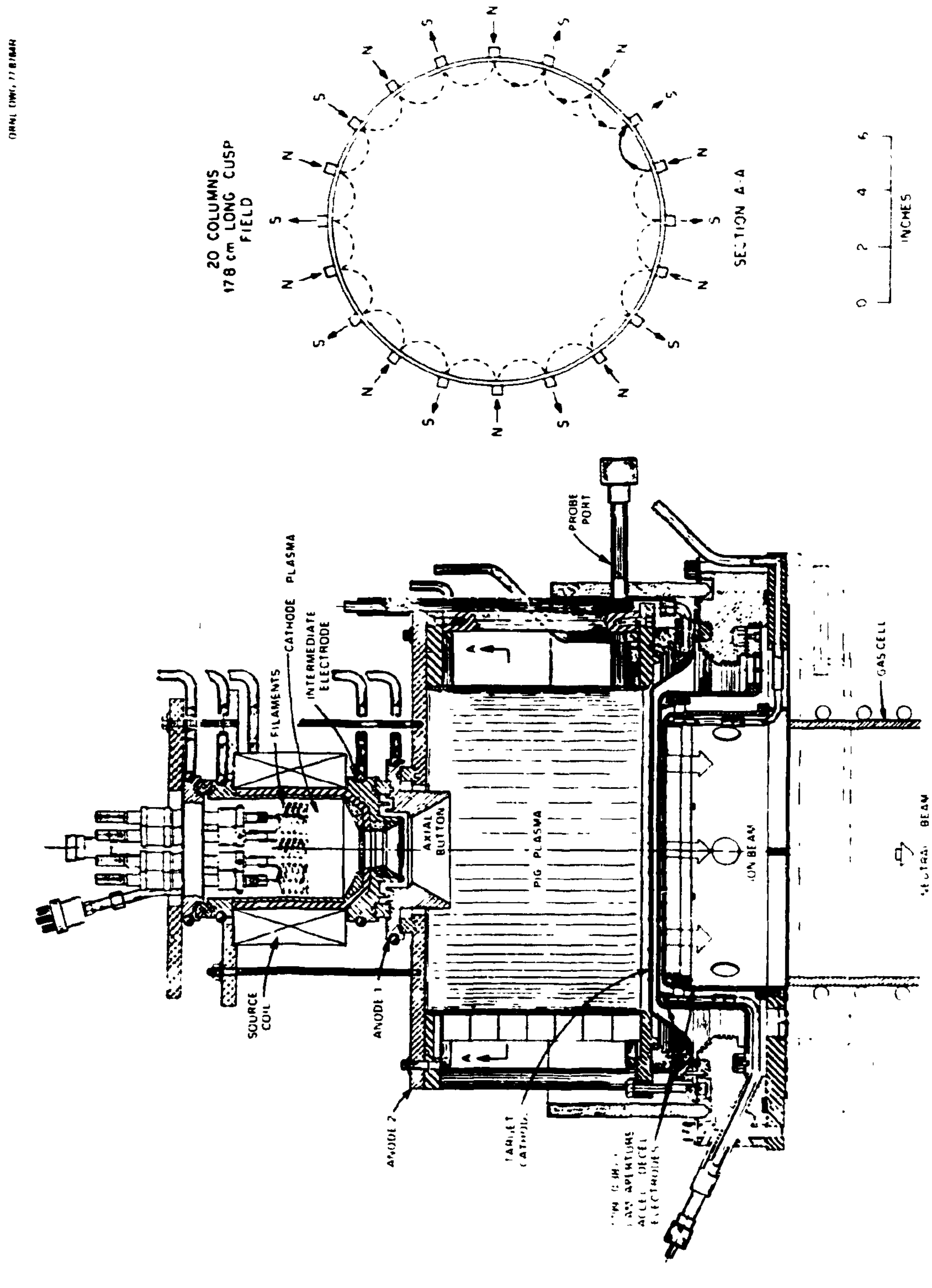
20 COLUMNS
17.8 cm LONG CUSP
FIELD
SECTION A-A
INCHES
PROBE PORT
CATHODE PLASMA
FILAMENTS
INTERMEDIATE ELECTRODE
AXIAL BUTTON
PIG PLASMA
SOURCE COIL
ANODE 1
ANODE 2
GAS CELL
ION BEAM

Figure 1

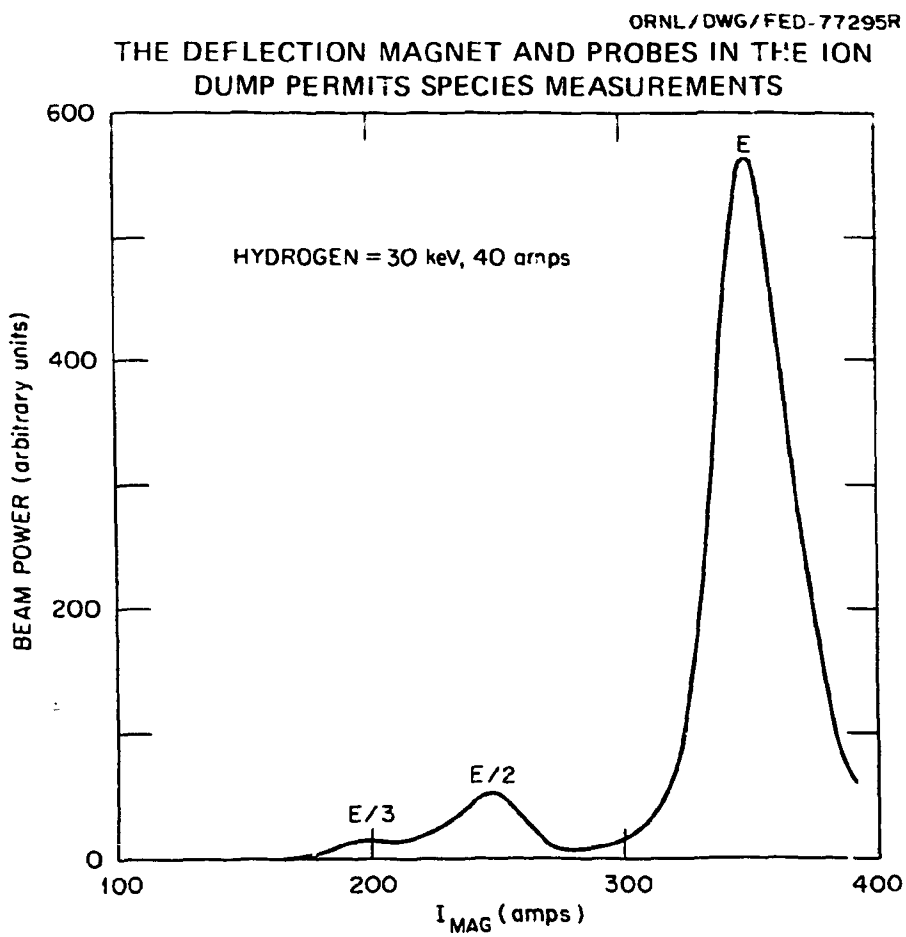
ORNL/DWG/FED-77295R
THE DEFLECTION MAGNET AND PROBES IN THE ION DUMP PERMITS SPECIES MEASUREMENTS
HYDROGEN = 30 keV, 40 amps
E
E/2
E/3
BEAM POWER (arbitrary units)
600
400
200
0
100
200
300
400
I MAG (amps)

Figure 2

Table 1. Source performance of PLT injector

Neutral power	750 kW
Beam energy	45 keV
Beam current	70 A
Pulse duration	∿500 ms
Arc voltage	<150 V
Arc current	<900 A
Arc efficiency	∿0.9 kW/A
Gas	Hydrogen
Gas efficiency	>50%
Proton yield	∿85%
Beam divergence	$\theta_{HWHM} \approx 1°$
Reliability	>90%

Table 2. Arc condition of 22-cm-modified duoPIGatron

Working gas	Hydrogen
Gas pressure	$\sim$100 mTorr, IE chamber
	$\sim$15 mTorr, TC region
Arc voltage	Up to 150 V
Arc current	Up to 900 A
Magnetic field	$\sim$200–300 G, IE region
	$\sim$10– G, TC region
Electrode potential	$^{a}V_F \cong 0$
	$^{b}V_{IE} = \sim$20–40 V
	$^{c}V_{TC} = \sim$60–120 V
	$^{d}V_a \simeq \sim$80–150 V
Plasma uniformity	$\sim\pm$5% over 22-cm grid
Plasma density	Up to 2×10^{12} cm^{-3} at extraction surface
Electron temperature	$\sim$5 eV

$^{a}V_{IE}$ is Intermediate Electrode (IE) potential

$^{b}V_{TC}$ is Target Cathode (TC) potential

$^{c}V_F$ is Filament (or arc negative) potential

$^{d}V_a$ is Anode potential

Table 3. Dominant reactions

Reactions	σ (10^{-16} cm^2)	E (eV)	$\langle\sigma v\rangle$ (10^{-8} cm^3/s)	n_a (10^{14} cm^{-3})	n_b (10^{10} cm^{-3})	$n_a n_b \langle\sigma v\rangle$ (10^{16} cm^{-3} s^{-1})
Ionization of H_2						
$H_2 + e_h(E) \rightarrow H_2^+ + 2e$	0.96	70	4.8	6	4	115
Dissociation of H_2						
$H_2 + e_c(E) \rightarrow 2H_1 + e$		3	0.03	6	9×10^2	162
Dissociative excitation of H_2^+						
$H_2^+ + e_c(E) \rightarrow H_1^+ + H_1 + e$		3	5	1.2×10^{-2}	9×10^2	54
Dissociative recombination of of H_2^+						
$H_2^+ + e_c(E) \rightarrow 2H_1$	3	3	3	1.2×10^{-2}	9×10^2	32
Total H_1^+ production from H_2^+						
$H_2^+ + e_c(E) \rightarrow H_1^+$	6	3	6.3	1.2×10^{-2}	9×10^2	67.5
Ionization of H_1						
$H_1 + e_h(E) \rightarrow H_1^+ + 2e$	0.7	70	3.5	0.5	4	7.0
Excitation and ionization of H_1						
$H_1 + e_h \rightarrow H_1^*(2p) + e$	0.7	70	3.5	0.5	4	7.0
$H_1^*(2p) + e_c(E) \rightarrow H_1^+ + 2e$	7	4	8.4	9.2×10^{-3}	$9 \times 10^{[illegible]}$	7.0
Charge exchange of H_2^+						
$H_2^+ + H_2 \rightarrow H_3^+ + H_1$	40	0.1	0.05	6	$1.2 \times 10^{[illegible]}$	36
Dissociative recombination of H_3^+						
$H_3^+ + e_c(E) \rightarrow 3H_1$	5	3	4.2	0.8×10^{-2}	[illegible] $\times 10^{[illegible]}$	30

ORNL/TM-6360
Dist. Category UC-20 a

INTERNAL DISTRIBUTION

1. G. C. Barber
2. C. F. Barnett
3. L. A. Berry
4. C. W. Blue
5. J. D. Callen
6. W. K. Dagenhart
7. R. A. Dandl
8. R. C. Davis
9. C. A. Foster
10. W. L. Gardner
11. H. H. Haselton
12. T. C. Jernigan
13. G. G. Kelley
14. J. Kim
15. M. S. Lubell
16. M. M. Menon
17. H. C. McCurdy
18. S. L. Milora
19. O. B. Morgan
20. N. S. Ponte
21. M. Roberts
22. M. W. Rosenthal
23. P. M. Ryan
24. D. E. Schechter
25. S. W. Schwenterly
26. J. Sheffield
27. D. Steiner
28. W. L. Stirling
29-58. C. C. Tsai
59. J. H. Whealton
60. R. E. Wright
61-62. Central Research Library
63. Document Reference Section
64-65. Laboratory Records
66. Laboratory Records, ORNL-RC
67. ORNL Patent Office
68-69. Fusion Energy Division Library
70. Fusion Energy Division Communications Center

EXTERNAL DISTRIBUTION

71. D. J. Anthony, Energy Systems and Technology Division, General Electric Company, 1 River Road, Bldg. 23, Room 2, Schenectady, NY 12345
72. C. Baker, Argonne National Laboratory, 9700 South Cass Avenue, Argonne, IL 60439
73. J. W. Beal, General Atomic Company, P.O. Box 608, San Diego, CA 92112
74. J. F. Clarke, Office of Fusion Energy (ETM), U.S. Department of Energy, Washington, DC 20545
75. F. E. Coffman, Office of Fusion Energy (ETM), U.S. Department of Energy, Washington, DC 20545
76. R. W. Conn, Department of Nuclear Engineering, University of Wisconsin, Madison, WI 53706
77. S. O. Dean, Office of Fusion Energy (ETM), U.S. Department of Energy, Washington, DC 20545
78. H. P. Eubank, Plasma Physics Laboratory, Princeton University, P.O. Box 451, Princeton, NJ 08540
79. T. K. Fowler, Lawrence Livermore Laboratory, University of California, P.O. Box 808, Livermore, CA 94550
80. H. K. Forsen, Exxon Nuclear Company, 2955 George Washington Way, Richland, WA 99352
81. H. P. Furth, Plasma Physics Laboratory, Princeton University, P.O. Box 451, Princeton, NJ 08540
82. R. W. Gould, Electrical Engineering and Physics Department, Bldg. 116-81, California Institute of Technology, Pasadena, CA 91109

BLANK PAGE

84. Ray Huse, Chairman, EPRI Fusion Program Committee, Public Service Electric and Gas Company, 80 Park Place, Newark, NJ 07101
85. E. E. Kintner, Office of Fusion Energy (ETM), U.S. Department of Energy, Washington, DC 20545
86. S. Matsuda, Japan Atomic Energy Research Institute, Tokai, Ibaraki, Japan
87. Director, Max Planck Instituut für Plasmaphysik, Garching bei München, Federal Republic of Germany
88. G. H. Miley, Nuclear Engineering Program, University of Illinois, Urbana, IL 61801
89. T. Ohkawa, General Atomic Company, P.O. Box 608, San Diego, CA 92112
90. R. V. Pyle, Lawrence Berkeley Laboratory, University of California, Berkeley, CA 94120
91. D. J. Rose, Massachusetts Institute of Technology, James Forrestal Campus, Cambridge, MA 02139
92. N. N. Semasko, Kurchatov Atomic Energy Institute, Moscow, U.S.S.R.
93. T. Sluyters, Brookhaven National Laboratory, Upton, Long Island, NY 11973
94. H. S. Staten, Office of Fusion Energy (ETM), U.S. Department of Energy, Washington, DC 20545
95. L. D. Stewart, Plasma Physics Laboratory, Princeton University, P.O. Box 451, Princton, NJ 08540
96. E. Thompson, Culham Laboratory, Abingdon, Oxfordshire, United Kingdom
97. F. Valckx, Centre d'Études Nucléaires, B.P. No. 6, Fontenay-aux-Roses, France
98. J. M. Williams, Office of Fusion Energy (ETM), U. S. Department of Energy, Washington, DC 20545
99. J. T. Woo, Massachusetts Institute of Technology, James Forrestal Campus, Cambridge, MA 02139
100. Director, Research and Technical Support Division, U.S. Department of Energy, Oak Ridge Operations, P.O. Box E, Oak Ridge, TN 37830

101-249. Given distribution as shown in TID-4500, Magnetic Fusion Energy (Distribution Category UC-20 a, Plasma Systems)